Local phosphocycling mediated by LOK/SLK restricts ezrin function to the apical aspect of epithelial cells

Raghuvir Viswanatha, Patrice Y. Ohouo, Marcus B. Smolka, and Anthony Bretscher

Department of Molecular Biology and Genetics, Weill Institute for Cell and Molecular Biology, Cornell University, Ithaca, NY 14853

In this paper, we describe how a dynamic regulatory process is necessary to restrict microvilli to the apical aspect of polarized epithelial cells. We found that local phosphocycling regulation of ezrin, a critical plasma membrane–cytoskeletal linker of microvilli, was required to restrict its function to the apical membrane. Proteomic approaches and ribonucleic acid interference knockdown identified lymphocyte-oriented kinase (LOK) and SLK as the relevant kinases. Using drug-resistant LOK and SLK variants showed that these kinases were sufficient to restrict ezrin function to the apical domain. Both kinases were enriched in microvilli and locally activated there. Unregulated kinase activity caused ezrin mislocalization toward the basolateral domain, whereas expression of the kinase regulatory regions of LOK or SLK resulted in local inhibition of ezrin phosphorylation by the endogenous kinases. Thus, the domain-specific presence of microvilli is a dynamic process requiring a localized kinase driving the phosphocycling of ezrin to continually bias its function to the apical membrane.

Introduction

Essentially, all cells are functionally polarized, a property requiring compositionally distinct regions of the plasma membrane. Not only is the composition distinct, but the morphology can also be highly domain specific. The apical aspect of epithelial cells is characterized by the presence of abundant microvilli, but how these are restricted to this domain is unknown. The F-actin membrane–linking protein ezrin functions specifically at the apical domain to regulate microvilli. Here, we show how ezrin is regulated to bring about this domain specificity.

Ezrin is the founding member of the ezrin-radixin-moesin (ERM) family of proteins and a functionally important component of microvilli (Fehon et al., 2010). In support of this role, cultured epithelial cells with reduced ERM protein expression lack microvilli (Takeuchi et al., 1994; Bonilha et al., 1999), and microvilli in the ezrin knockout mouse are short and misformed (Bonilha et al., 2006). The ERM proteins are conformationally regulated: in their closed, inactive state, the N-terminal 4.1 ERM (FERM) domain is tightly bound to the C-terminal tail (Gary and Bretscher, 1995). Upon the concerted action of the plasma membrane phospholipid phosphatidylinositol 4,5-bisphosphate and kinases that phosphorylate a C-terminal threonine residue (threonine 567 [T567] ezrin/T564 radixin/T558 moesin), this intramolecular interaction is disrupted by electrostatic repulsion (Hirao et al., 1996; Nakamura et al., 1996; Matsui et al., 1998; Pietromonaco et al., 1998; Simons et al., 1998; Gautreau et al., 2000; Pearson et al., 2000; Fievet et al., 2004). In the open conformation, binding sites for transmembrane- and membrane-associated proteins in the FERM domain and an F-actin binding site in the C-terminal tail become unmasked and thereby reveal the membrane–cytoskeletal linking function of the protein (Fehon et al., 2010).

After the discovery of ERM C-terminal phosphorylation (Nakamura et al., 1996), Rho-associated kinase was initially thought to phosphorylate ERMs in microvilli (Matsui et al., 1998), but this has been questioned (Matsui et al., 1999), and several other ERM kinases have since been proposed. These include the myotonic dystrophy kinase-related Cdc42-binding kinase (Nakamura et al., 2000) and isoforms of protein kinase C (Pietromonaco et al., 1998; Ng et al., 2001) in fibroblasts; in epithelial cells, the Ste20-like kinase 4 (MST4; ten Klooster

Correspondence to Anthony Bretscher: apb5@cornell.edu

Abbreviations used in this paper: EGFR, EGF receptor; ERM, ezrin-radixin-moesin; FERM, 4.1 ERM; IBR, integrin-binding region; LOK, lymphocyte-oriented kinase; pERM, phospho-ERM.

The Rockefeller University Press $30.00
J. Cell Biol. Vol. 199 No. 6 969–984
www.jcb.org/cgi/doi/10.1083/jcb.201207047

et al., 2009; Fidalgo et al., 2012); and in lymphocytes, the lymphocyte-oriented kinase (LOK; Belkina et al., 2009). This apparent complexity has hampered study of the contribution of individual kinases that regulate ERM protein function. In contrast, in *Drosophila melanogaster*, the kinase Slik has been shown to phosphorylate the sole ERM orthologue moesin in tissue culture cells and in situ (Hipfner et al., 2004; Hughes and Fehon, 2006; Carreno et al., 2008; Kunda et al., 2008).

Here, we examine the dynamics of ezrin phosphorylation in human epithelial cells and show that cycling of T567 phosphorylation is required to restrict ezrin function to the apical membrane. Using proteomic approaches, we identify the related kinases LOK and SLK (Ste20-like kinase), homologues of *Drosophila* Slik, as the major contributors to ezrin activation in two epithelial cell lines. Moreover, we show that the kinases themselves are components of apical microvilli, and their local activation is required for the polarized distribution of ezrin.

Results

Ezrin undergoes rapid T567 phosphorylation cycling

T567 is the major site of phosphorylation regulating ezrin activation, yet the fraction of the protein phosphorylated in epithelial cells has not been explored. Using Phos-tag gels (Kinoshita et al., 2006), in which the mobility of phosphorylated proteins is specifically retarded, ezrin from the microvilli-decorated Jeg-3 epithelial cell line resolves into two species of approximately equal abundance (Fig. 1 A). The slower migrating band is selectively recognized by an antibody specific for ERM C-terminal threonine phosphorylation (phospho-ERM [pERM]) and is absent from expressed T567A ezrin (Fig. S1, A and B). The cell-permeable phosphatase inhibitor calyculin A is known to reduce ezrin dephosphorylation (Chen et al., 1995), so we explored whether treatment enhances the relative abundance of ezrin T567 phosphorylation. 5-min treatment with 1 µM calyculin A resulted in essentially complete ezrin phosphorylation (Fig. 1 A). These results show that about half of the ezrin is phosphorylated in these cells, and the other half can be rapidly phosphorylated in vivo in the absence of opposing phosphatase activity.

To explore the dynamics of phosphorylation of ezrin on T567 in more detail, we followed the extent of phosphorylation as a function of time after adding either the general kinase inhibitor staurosporine (1 µM) or calyculin A (1 µM). Of the ERM proteins, Jeg-3 cells express ezrin and radixin, which have an identical sequence in the region of ezrin T567, so the antibody detects the phosphorylated state of both proteins. In all experiments, the percentage of ezrin and radixin that is phosphorylated is similar, so we considered them together. Quantitative Western blotting with the pERM antibody was used to determine the degree of C-terminal threonine phosphorylation. The lifetime of the dephosphorylated species in the presence of phosphatase inhibitor and that of the phosphorylated species in the presence of kinase inhibitor were each ~2 min (Fig. 1, B and C). The results show that ezrin and radixin undergo constant C-terminal phosphocycling in vivo.

Ezrin phosphocycling is necessary for ezrin localization to microvilli

We next explored whether the T567E phosphomimetic mutant of ezrin or the T567A phosphodeficient mutant localizes appropriately. Numerous previous studies have used a C-terminal tag to follow expressed ezrin (e.g., Crepaldi et al., 1997; Yonemura et al., 1999; Gautreau et al., 2000; Dard et al., 2001; Coscoy et al., 2002; Karagiosis and Ready, 2004). However, as the C terminus makes important contacts with the FERM domain to maintain an inhibited conformation (Pearson et al., 2000), we were concerned that a C-terminal tag might affect the regulation of the protein. We therefore explored the possibility of introducing an internal tag and chose a region between the α-helical ERM coiled coil and the tail that is not ordered in the x-ray structure and also poorly conserved within the ERM family (Fig. S1 C; Li et al., 2007). Expression of an ezrin construct in which the eight residues of the Flag epitope replaced eight residues in the disordered region colocalized precisely with endogenous radixin similarly to endogenous ezrin (Fig. 2 A). We therefore used ezrin with this internal tag, ezrin-iFlag, for many of our subsequent experiments.

Jeg-3 cells that stably express wild-type ezrin-iFlag, phosphodeficient ezrin-T567A-iFlag, or the phosphomimetic ezrin-T567E-iFlag were generated. In all cases, the level of expression was about the same as endogenous ezrin (Fig. S1 D). Ezrin-T567A-iFlag could not be detected in microvilli and showed dim fluorescence in the cytoplasm (Fig. 2 A). Unexpectedly, ezrin-T567E-iFlag was poorly concentrated in microvilli, with the vast majority mislocalized all over the plasma membrane, including to the basolateral membrane, a site where wild-type ezrin is never enriched, and importantly without disturbing the apical localization of radixin (Fig. 2 A). To see whether this is a general property of open ezrin mutants, we also explored the localization of ezrin-1–583-iFlag and ezrin-1–479-Flag, in which the C-terminal tail of ezrin is truncated or deleted, and ezrin N mutant-iFlag, which is open because of a mutation in the FERM domain that blocks binding to its otherwise functional C-terminal tail (Finnerty et al., 2004; Chambers and Bretscher, 2005). All constructs localized more generally to the plasma membrane than wild-type ezrin-iFlag, and none affected the localization of radixin (Fig. 2 B).

To explore the effect of stable C-terminal threonine phosphorylation of endogenous ezrin, we examined the localization of ezrin after brief calyculin A treatment. This resulted in the localization of ezrin not only in microvilli but also generally to the plasma membrane, including the basolateral membrane (Fig. 2 C). Collectively, these results imply that phosphocycling of ezrin regulates its distribution by controlling its open state.

Phosphoregulatory control of ezrin localization is necessary for microvilli formation

As our data show that ezrin hyperphosphorylation resulting from phosphatase inhibition results in partial mislocalization, we wished to determine whether T567 phosphocycling is necessary for microvilli formation. Microvilli are found on 70–80% of Jeg-3 cells, and their presence is almost entirely dependent

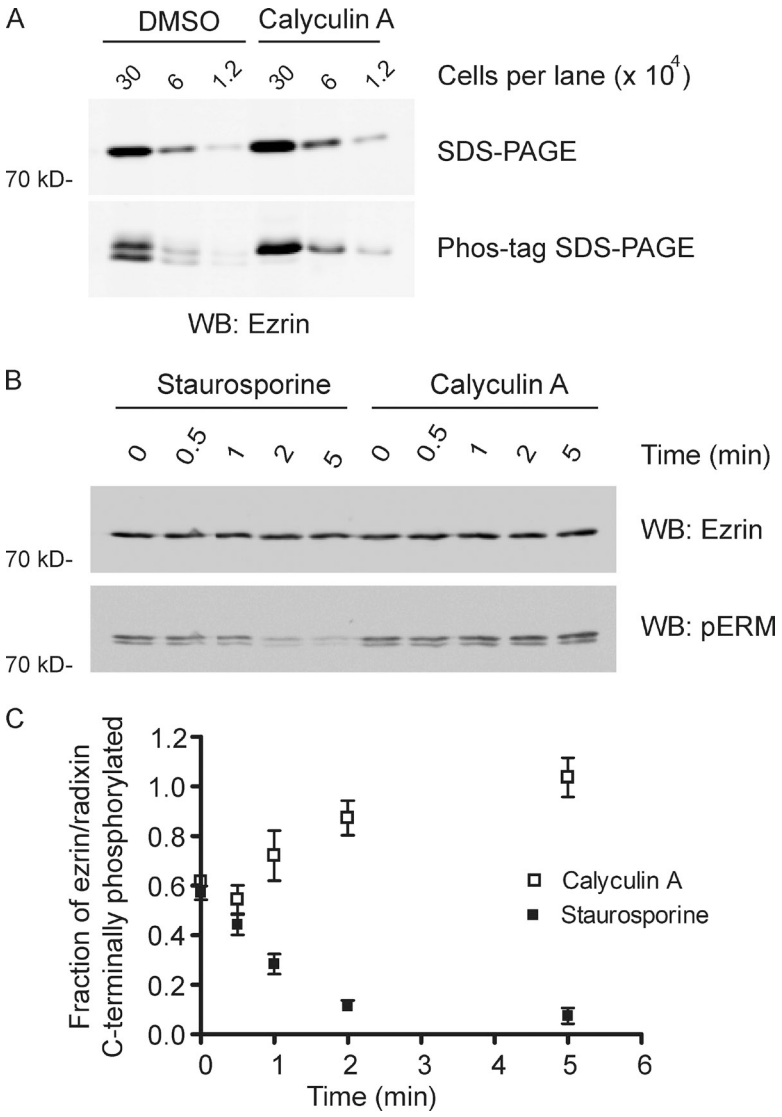

Figure 1. **Half of ezrin is phosphorylated, and phosphoezrin has a turnover time of ∼2 min.** (A) A fivefold dilution series of lysates of Jeg-3 cells treated as indicated was resolved by SDS-PAGE with or without Phos-tag and Western blotted for ezrin. The abundance of phosphorylated and nonphosphorylated ezrin is nearly equal; ezrin is nearly quantitatively phosphorylated after treatment with calyculin A for 5 min. (B) Time course of treatment of cells with 1 µM staurosporine or 1 µm calyculin A on the level of phospho-ERM (pERM) and total ezrin as seen by Western blotting. (C) Quantification of data in B from three independent experiments. Means ± SD are shown. WB, Western blot.

on ezrin and radixin (unpublished data). Depletion of ezrin alone by siRNA reduces the number of cells expressing abundant microvilli to ∼45%, with some microvilli remaining over regions of cell–cell contact (Fig. 3, A and B), as is also seen when the microvillar component EBP50 (ERM-binding phosphoprotein 50 kD) is depleted (Hanono et al., 2006; Garbett et al., 2010). Therefore, this provides a system to ask whether phosphomimetic variants of ezrin can contribute to the formation of microvilli. Jeg-3 cells stably expressing siRNA-resistant untagged wild-type ezrin, ezrin-T567A, or ezrin-T567E at near-endogenous ezrin levels were generated, and all were found to have microvilli as seen by radixin staining. Endogenous ezrin was then depleted in these cells by siRNA treatment, and the presence of microvilli was scored (Fig. 3 B). Whereas expression of wild-type ezrin completely restored the presence of microvilli, neither ezrin-T567A nor ezrin-T567E was able to bring back microvilli.

We also examined the functionality of the widely used C-terminally tagged GFP constructs. In contrast to untagged or internally tagged ezrin-T567A, we found that ezrin-T567A-GFP is membrane-targeted, consistent with our concern that it might be slightly activated. Nonetheless, neither siRNA-resistant T567A nor T567E in the context of ezrin-GFP rescued microvilli, whereas siRNA-resistant wild-type ezrin-GFP rescued microvilli in the absence of endogenous ezrin (Fig. S1, E and F). We conclude that although ezrin-GFP may be partially activated relative to untagged ezrin, it still requires phosphocycling to perform its function in microvillus biogenesis. Collectively, these results indicate that the precise spatial control of ezrin phosphocycling is necessary for microvilli.

LOK and SLK are the major kinases involved in ezrin phosphorylation

We used mass spectrometry of ezrin immunoprecipitates to identify the kinases in Jeg-3 cells responsible for phosphorylating ezrin. To identify transient ezrin-interacting kinases with high sensitivity, we used a cross-linking strategy together with the stable isotope labeling of amino acids in cell culture procedure (Ong et al., 2002) to compare ezrin-iFlag immunoprecipitates to control immunoprecipitates. Although >18 kinases were identified, the four enriched more than twofold in ezrin-iFlag immunoprecipitates are shown in Fig. 4 A. The most highly enriched serine/threonine kinases were the evolutionary

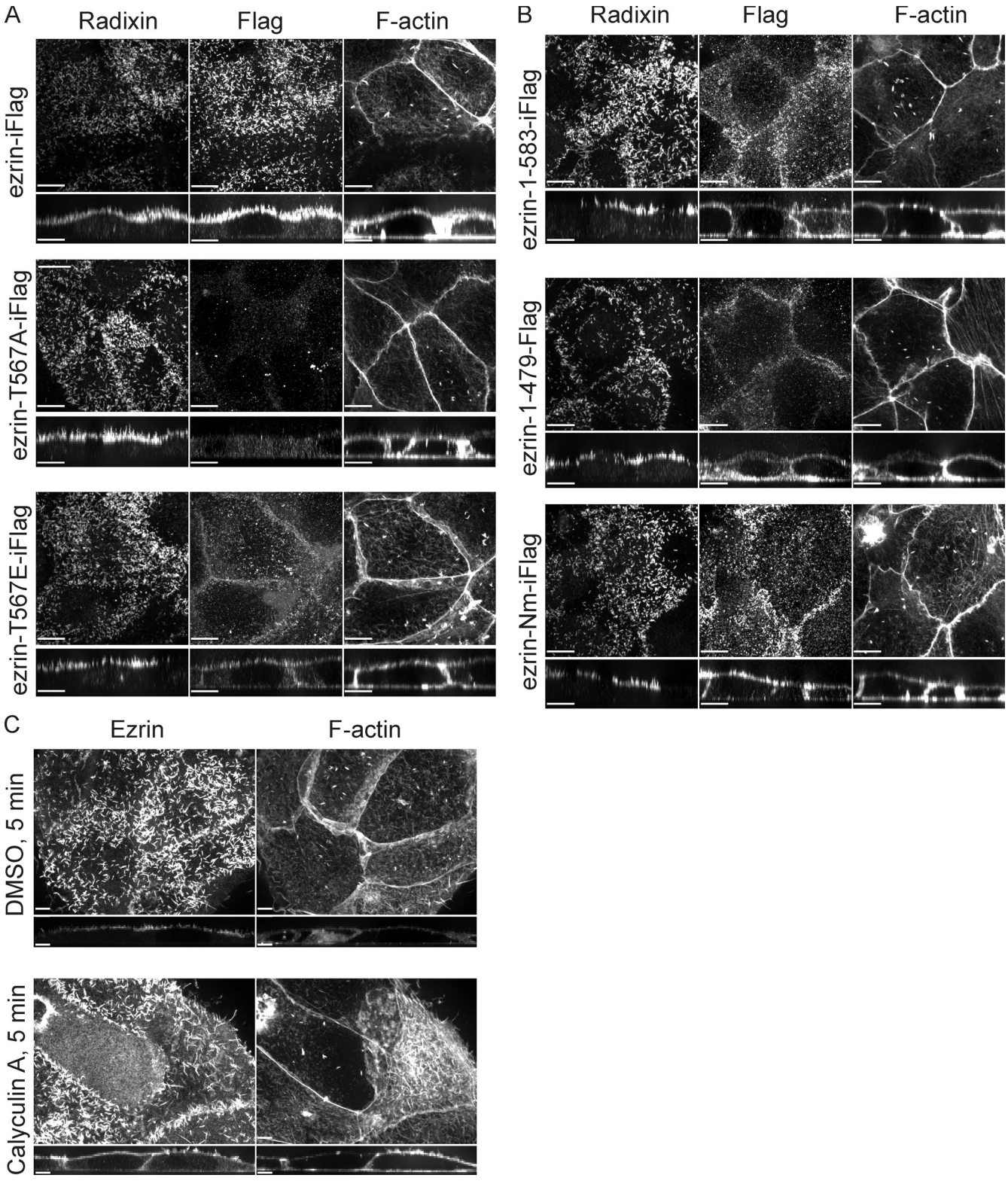

Figure 2. **Constitutively open ezrin loses apical versus basal polarity.** (A) Jeg-3 cells expressing ezrin-iFlag or its T567 phosphomutants (Fig. S1, C and D) were stained using a Flag antibody, and the localization was compared with endogenous radixin and F-actin. For every sample, a maximum intensity projection of the apical surface en face as well as a vertical cross section is shown. (B) Cells stably expressing ezrin C-terminal truncation mutants or the N mutant (Nm), all of which are known to be constitutively open, were processed and imaged as in A. Compromising the FERM–C terminus interaction in ezrin reduces ezrin-iFlag accumulation in microvilli, without affecting the polarized distribution of radixin. (C) Cells were treated with DMSO or 0.1 µM calyculin A for 5 min, and ezrin and F-actin were localized. Calyculin A treatment causes ezrin to mislocalize. Bars, 10 µm. Vertical sections were expanded fivefold in z for clarity.

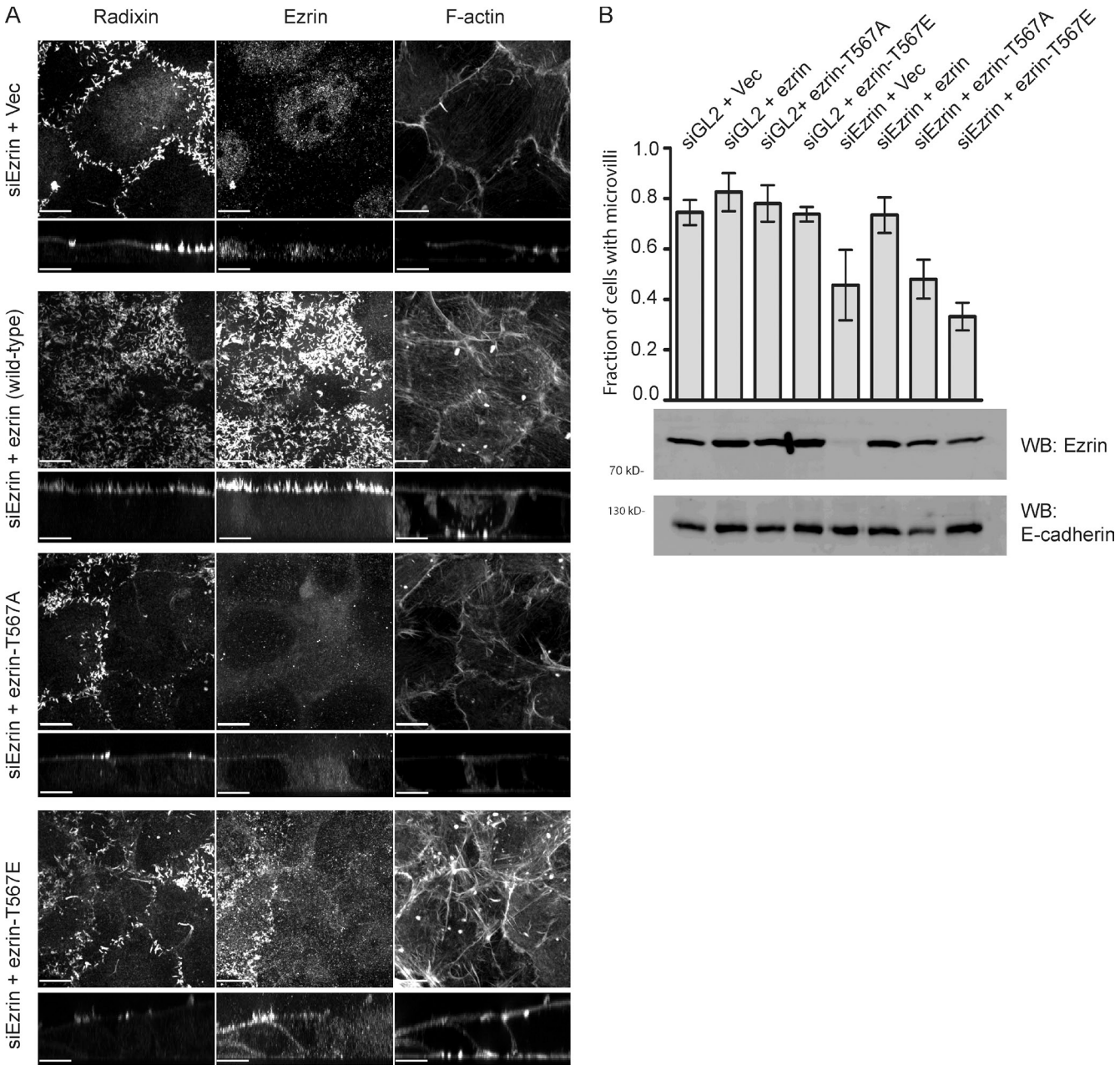

Figure 3. **Phosphomimetic, activated ezrin cannot rescue microvilli when endogenous ezrin is depleted by RNAi.** (A) Cells stably expressing the indicated ezrin protein or vector (Vec) control were treated for 3 d with siRNA to deplete endogenous ezrin, and microvilli were revealed by radixin and F-actin staining. (B) Quantification of the presence of microvilli as reported by radixin or F-actin staining. Wild-type ezrin but neither phosphodeficient nor phosphomimetic ezrin restores microvilli after knockdown of endogenous ezrin. Data in B are means ± SD of four independent experiments, and >150 cells were scored per treatment in each experiment. Bars, 10 µm. Cross sections were expanded fivefold vertically for clarity. WB, Western blot.

homologues LOK and SLK (Delpire, 2009). Immunoprecipitation of ezrin-iFlag coprecipitates some LOK-GFP (Fig. 4 B) and some endogenous LOK (Fig. S2 B), thereby supporting the mass spectrometry results.

If LOK and SLK are the relevant kinases for ezrin phosphorylation, we would expect the level of T567 phosphorylation to decrease when the level of LOK and/or SLK is reduced. Depletion of LOK by siRNA treatment resulted in about a 50% decrease in T567 phosphorylation (Fig. 4 C). This effect of LOK siRNA was corroborated with a second LOK-specific siRNA (Fig. S2 C). SLK depletion had a minimal effect on T567 phosphorylation, but importantly, knocking down both LOK and SLK reduced ezrin T567 phosphorylation even further to ∼20% of control levels (Figs. 4 C and S2 C), implying that ezrin is a substrate of both LOK and SLK in these cells. Jeg-3 cells also express MST4 and MINK1, two kinases that phosphorylate ezrin (ten Klooster et al., 2009), but validated siRNAs against these kinases had no effect on the level of ezrin phosphorylation (Fig. S2 C). Furthermore, Rho-associated kinase inhibitor Y-27632 and Cdk inhibitor roscovitine had no effect on T567 phosphorylation in Jeg-3 cells (unpublished data). Consistent with a major role for LOK, fewer cells knocked

A

Serine/Threoine Kinase	# of peptides recovered	Enrichment on Ezrin-iFlag
STK10/LOK	13	4.0
SLK	9	3.6
CDK1	7	2.6
MINK1	2	2.1

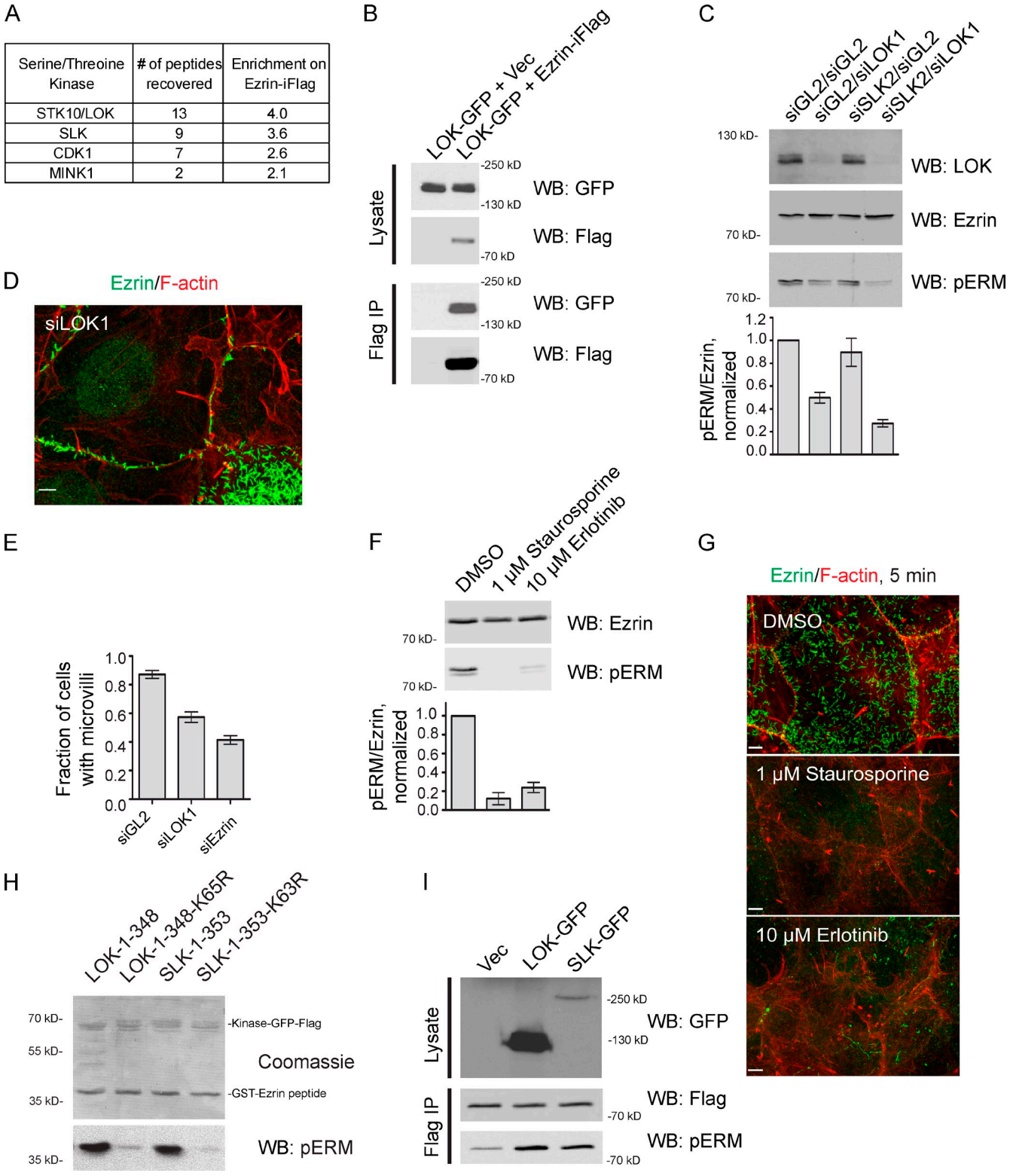

Figure 4. **LOK and SLK are responsible for ezrin/radixin C-terminal phosphorylation in Jeg-3 cells.** (A) Enrichment statistics for top four kinases identified by mass spectrometry analysis of ezrin-iFlag cross-linking immunoprecipitates. LOK and SLK were the most highly enriched serine/threonine kinases binding to ezrin-iFlag. (B) LOK-GFP was coexpressed with empty vector or ezrin-iFlag, and cells were subjected to cross-linking immunoprecipitation using anti-Flag (Flag IP). LOK-GFP coimmunoprecipitates with ezrin-iFlag. (C) Cells were treated with the indicated combinations of validated siRNAs against LOK (siLOK1), SLK (siSLK2), or control (siGL2) and Western blotted for LOK to measure knockdown efficiency. The level of phosphorylated ezrin and radixin was determined by Western blotting and quantified by densitometry. (D) Cells were treated with siLOK1 for 3 d and then fixed and stained for ezrin and F-actin. Knockdown of LOK causes loss of microvilli similar to the knockdown of ezrin (Fig. 3 A). (E) The presence of microvilli on cells treated with the indicated siRNA was assessed after ezrin and F-actin staining. (F) Cells were treated with DMSO, staurosporine, or erlotinib at the indicated concentrations for 5 min at 37°C, and pERM levels were measured by Western blotting. (G) Cells treated as in F were fixed and stained for ezrin and F-actin. Erlotinib treatment causes a severe reduction in ezrin-containing microvilli. (H) GFP-Flag–tagged kinase constructs were immunoprecipitated using the Flag tag after expression in

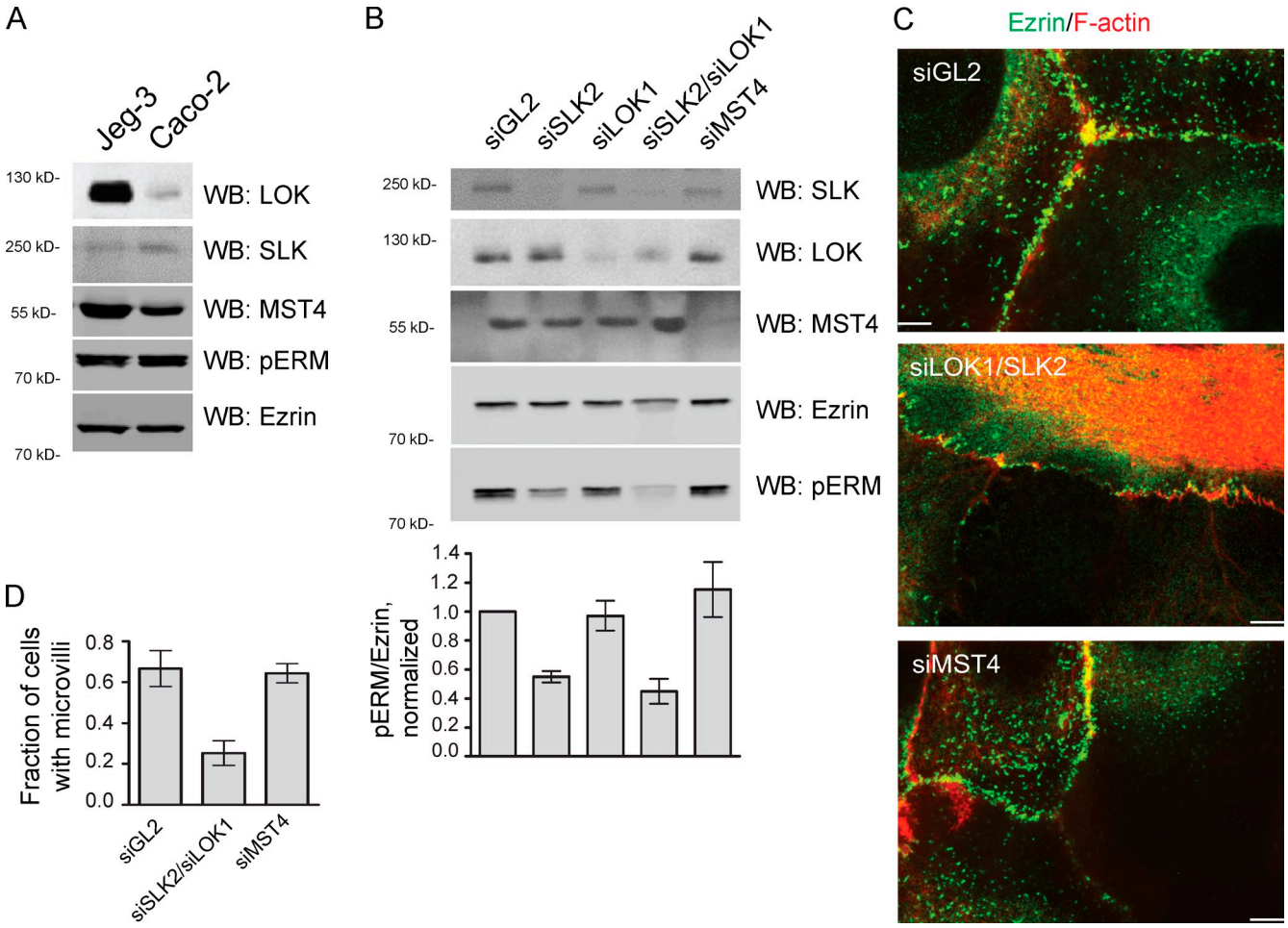

Figure 5. **LOK and SLK are necessary for ERM phosphorylation in Caco-2 cells.** (A) Western blots of equivalent numbers of Jeg-3 or Caco-2 cells for LOK, SLK, MST4, pERM, and ezrin as indicated. (B) Caco-2 cells transfected with indicated siRNAs were Western blotted for phospho-ERM (pERM) and total ezrin and quantified by densitometry. (C) Caco-2 cells transfected with indicated siRNAs were fixed and stained for ezrin and F-actin. (D) Caco-2 cells were scored for presence or absence of microvilli by F-actin stain. Data in B and D are means ± SD of three or four independent experiments. WB, Western blot. Bars, 10 µm.

down for LOK exhibited microvilli on their apical surface (Fig. 4, D and E), an effect similar to that seen when ezrin is depleted by siRNA (Fig. 3).

Erlotinib, a small molecule inhibitor of the EGF receptor (EGFR) tyrosine kinase, was recently shown to inhibit LOK and SLK when used at higher concentrations (Yamamoto et al., 2011). A 5-min treatment with 10 µM erlotinib resulted in the loss of ezrin phosphorylation and loss of microvilli from Jeg-3 cells, similar to 1 µM of the general kinase inhibitor staurosporine (Fig. 4, F and G).

Functional but not kinase-dead LOK or SLK kinase domains could each phosphorylate T567 in the context of the C-terminal domain of ezrin in vitro (Fig. 4 H). Moreover, overexpression of LOK-GFP or SLK-GFP increased the phosphorylation of cotransfected ezrin-iFlag in vivo (Fig. 4 I). Collectively, our results show that LOK and SLK are functionally the major relevant kinases involved in the steady-state phosphorylation of ezrin in Jeg-3 cells.

LOK/SLK are the general epithelial cell ERM kinases

We next asked whether LOK and SLK C-terminally phosphorylate ERMs in other epithelial cells in addition to their role in placentally derived Jeg-3 cells, by examining ERM phosphorylation in colon-derived Caco-2 cells. Just as with Jeg-3, Caco-2 cells express ezrin and radixin but no moesin. Interestingly, Caco-2 cells express slightly more SLK and much less LOK than Jeg-3 cells, but steady-state ezrin and radixin C-terminal phosphorylation is nearly identical (Fig. 5 A). This suggests that SLK is more active than LOK in these cells.

HEK293T cells and then combined with purified GST-tagged ezrin C terminus in the presence of ATP, which was then subjected to pERM Western blotting. Both LOK and SLK kinase domains are able to phosphorylate the ezrin C-terminal tail in vitro. (I) Cells were cotransfected with an empty vector or GFP fusions of either LOK or SLK along with ezrin-iFlag. The cells were lysed, ezrin-iFlag was immunoprecipitated with anti-Flag, and the phosphorylation of ezrin-iFlag was detected by Western blotting. Both LOK-GFP and SLK-GFP overexpression cause an increase in the overall level of ezrin-iFlag phosphorylation. Data in C, E, and F are means ± SD of three independent experiments. WB, Western blot; Vec, vector. Bars, 10 µm.

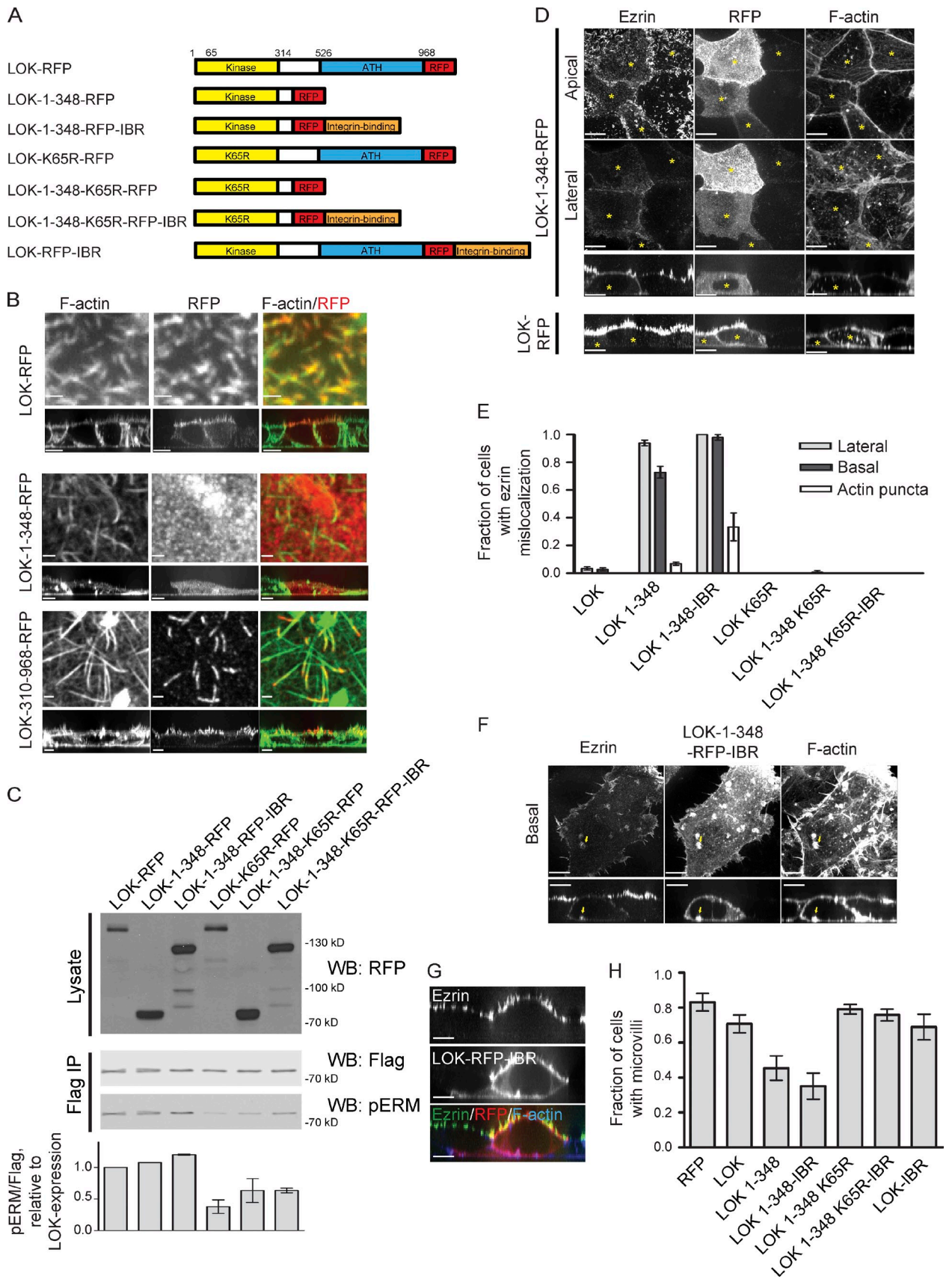

Figure 6. **Unregulated LOK causes ezrin depolarization.** (A) Schematic of truncation constructs and chimeras used. ATH, AT1-46 homology. (B) LOK-RFP and truncations were localized relative to F-actin. LOK and the LOK C-terminal domain localize to microvilli, whereas the N-terminal kinase domain does not. For clarity, only a small region of the apical domain is shown, and the full cell is shown in the vertical cross section. (C) Cells were cotransfected with

Consistently, siRNA-mediated depletion of SLK alone causes a 50% decrease in pERM level, whereas depletion of LOK has no measurable effect on its own (Fig. 5 B); however, combining LOK and SLK siRNAs revealed a marginal synergy between them ($P < 0.05$; Fig. 5 B). Depletion of MST4, the ERM kinase in the single polarized Ls174T-W4 cells (ten Klooster et al., 2009), had no effect on ezrin phosphorylation in Caco-2 (Fig. 5 B) or Jeg-3 cells (Fig. S2 B, right). An examination of Caco-2 cultures knocked down for LOK and SLK revealed a reproducible twofold loss of microvilli-bearing cells, whereas no such loss was observed when MST4 was depleted (Fig. 5 C). These results suggest that LOK and SLK are the general regulators of ERM phosphorylation in epithelial cells.

LOK activity is localized and restricted apically via the C-terminal domain

LOK has an N-terminal kinase domain and a C-terminal domain predicted to be similar to the AT1-46 homology domain of SLK (Figs. 6 A and S3 A; Sabourin et al., 2000). To dissect the molecular organization of LOK, we constructed a series of truncation mutants as well as generating the K65R kinase-dead mutant previously shown to inhibit LOK activity (Fig. 6 A; Belkina et al., 2009).

LOK has been shown to localize to the membrane of peripheral blood lymphocytes (Belkina et al., 2009), but a more precise location has not been reported. Although we were unable to localize endogenous LOK, LOK-RFP is mostly apical but also partially basolateral (Fig. 6 B). The N-terminal kinase domain failed to localize to any specific region, whereas low-level expression of the C-terminal domain localized specifically to apical microvilli (Fig. 6 B). Thus, LOK is localized to microvilli via the C-terminal domain.

To determine whether LOK distribution is important for its activity toward ezrin in vivo, we expressed truncations of LOK and their kinase-dead derivatives along with ezrin-iFlag and measured the effect on ezrin-iFlag phosphorylation (Fig. 6 C). Unexpectedly, we found that all constructs containing the active N-terminal kinase domain—even those that did not contain the C-terminal domain necessary for localization to microvilli—yielded a similar increase in ezrin-iFlag phosphorylation relative to constructs lacking kinase activity (Fig. 6 C).

Because the overexpression of either microvillus-localized LOK or the delocalized N-terminal kinase domain could both raise the level of phosphorylated ezrin to a similar extent (Fig. 6 C), this allowed us to explore the contribution of localizing the kinase activity to ezrin distribution. Cells overexpressing full-length LOK were unaffected: ezrin was still highly enriched in microvilli (Fig. 6 D). In contrast, cells overexpressing a delocalized kinase (LOK-1–348-RFP) consistently exhibited mislocalized ezrin including on the basolateral plasma membrane below cell–cell junctions, a location at which ezrin is never normally enriched (Fig. 6, D and E). This effect is caused by the mislocalized kinase activity because overexpression of either the kinase domain harboring the K65R mutation (LOK-1–348-K65R-RFP) or full-length LOK never caused ezrin to localize basolaterally (Fig. 6, D and E). Kinase-dead LOK-RFP (LOK-K65R-RFP) has a mild dominant-negative effect, reducing the number of cells with microvilli as discussed in the next section (Fig. 8 C), but the remaining ezrin did not mislocalize to basolateral membranes, consistent with a requirement for kinase activity in order for LOK constructs to have this effect. Delocalized ezrin was caused by delocalized ERM phosphorylation as seen by examining pERM distribution in the transfected cells (Fig. S3 B, top two rows). Overexpression of SLK or just the N-terminal kinase domain (1–353 aa) gave equivalent results to those obtained with LOK and its derivatives (Fig. S3, C–E). Collectively, these data suggest that LOK and SLK kinase activity must be apically restricted via the C-terminal domain to maintain microvilli.

We next asked whether intentionally mistargeting just the N-terminal kinase domain to a specific region of the basolateral membrane would cause ezrin to accumulate in that region. The C terminus of talin has been shown to bind integrins (Xing et al., 2001), so we generated a construct containing the LOK kinase domain fused to talin's integrin-binding region (IBR). Cells expressing the kinase domain IBR chimera (LOK-1–348-RFP-IBR) mislocalized ezrin on the basal plasma membrane as well as to basal actin puncta to a significantly greater extent than those expressing the kinase domain alone (LOK-1–348-RFP; Fig. 6, E [quantification] and F [arrows]). Therefore, ezrin enrichment coincides with the location of unregulated LOK activity.

Consistent with this and our earlier data showing that phosphomimetic ezrin cannot support microvillus formation, overexpression of a delocalized, active LOK kinase domain (LOK-1–348-RFP or LOK-1–348-RFP-IBR) greatly reduced the number of microvilli, whereas overexpression of full-length

indicated RFP-tagged LOK constructs along with ezrin-iFlag. The cells were lysed, ezrin-iFlag was immunoprecipitated (Flag IP), and phosphorylation of ezrin-iFlag was measured by quantitative Western blotting. The fold increase in ezrin phosphorylation as a result of each LOK truncation was normalized to the overexpression of full-length LOK. (D) Cells expressing the RFP-tagged LOK N-terminal kinase domain alone (LOK-1–348-RFP) were stained for ezrin and F-actin and presented as either an apical, basolateral, or side view, and cells transfected with full-length LOK-RFP (bottom) are presented in the side view. Cells expressing the LOK kinase domain alone exhibit delocalized ezrin staining, whereas cells expressing full-length LOK do not. (E) Cells expressing indicated LOK-RFP fusion proteins were stained as in D, and the ezrin depolarization phenotypes were quantified by confocal microscopy. Only when the LOK kinase domain is functional but unregulated does it cause ezrin to mislocalize. Note that although cells expressing LOK-K65R do not have mislocalized ezrin, fewer have microvilli, as reported in Fig. 8 C. (F) Cells overexpressing a fusion of the LOK kinase domain to the integrin-binding region (IBR) of talin were processed as in D. Arrows point to one F-actin–containing basal membrane–associated structure. When the kinase domain alone is intentionally mislocalized, ezrin is preferentially located around these structures. (G) Cell expressing full-length LOK fused to the IBR and stained for ezrin and F-actin. Even when intentionally mislocalized basally, full-length LOK does not cause ezrin to mislocalize, indicating that it is only active in the apical domain. (H) Cells expressing LOK-RFP and derivatives were stained with ezrin and F-actin, and the presence of microvilli was scored as in Figs. 3 B and 4 D. Active, mislocalized LOK constructs cause cells to lose microvilli. Data in B, E, and H are means ± SD of three or four independent experiments. Cross sections were expanded fivefold vertically for clarity, and yellow asterisks mark transfected cells. WB, Western blot. Bars: (B, En face images) 1 µm; (B [main images], D, F, and G) 10 µm.

LOK (LOK-RFP) did not (Fig. 6 G). Kinase activity was also required, because kinase-dead versions of the delocalized kinases (LOK-1–348-K65R-RFP or LOK-1–348-K65R-RFP-IBR) also failed to reduce microvilli (Fig. 6 G). Thus, the correct targeting and activation of LOK to microvilli by a mechanism involving its C-terminal domain is critical for the normal function and distribution of ezrin.

Overexpressed LOK was found to be partially mislocalized along basolateral membranes, but ezrin was never found associated with it (Fig. 6 D). Furthermore, when the full-length kinase was fused to the IBR (LOK-RFP-IBR), the chimera localized basolaterally to a greater extent, but ezrin remained strictly polarized in microvilli (Fig. 6 I), and microvilli remained intact (Fig. 6 H). Thus, in the context of the full-length protein, factors must exist that restrict LOK activity apically.

Localized LOK/SLK activity is sufficient for microvillus formation

To assess the importance of LOK and SLK in microvillus formation, we set out to generate erlotinib-resistant forms of the kinases. Erlotinib was first identified as an inhibitor of EGFR (Pao et al., 2005; Pao and Chmielecki, 2010). T766 of EGFR becomes mutated to methionine in some erlotinib-resistant cancers and has been shown to cause the occlusion of erlotinib from the ATP binding site (Pao et al., 2005). We asked whether the homologous mutation could be used to develop erlotinib-resistant LOK and SLK, which could then be used to test microvilli formation in the absence of endogenous LOK/SLK activity. Structural analysis revealed that the homologues of T766 in EGFR are I110 in LOK (Fig. S4 A) and I108 in SLK. Expression of LOK-I110M-GFP and SLK-I108M-GFP, but not a kinase-dead derivative, completely abrogated the loss of microvilli induced by erlotinib treatment (Figs. 7, A and B; and S4 B). Thus, LOK and SLK are each sufficient for localized ezrin phosphorylation leading to microvillus production.

Strikingly, expression of just the erlotinib-resistant LOK kinase domain failed to rescue microvillus loss in the presence of erlotinib (Fig. 7, B and C), even though the kinase domain was still able to restore ezrin and radixin phosphorylation after erlotinib treatment in the transfected cells (Fig. S4 C). Thus, regulation of LOK activity via the C-terminal domain is necessary for the presence of microvilli.

The LOK C-terminal domain both localizes and regulates the N-terminal kinase domain

To further investigate the localization of LOK activity, we examined the effect of expressing either full-length constructs or the C-terminal domain alone (Fig. 8 A). Low-level expression of the C-terminal domain of LOK (Fig. 6 B) or the equivalent region in SLK (Fig. S3 B, middle images) showed that it localizes preferentially to microvilli. Strikingly, however, high-level expression of the entire LOK C-terminal domain (residues 310–968) or a smaller segment (residues 586–968) caused a significant reduction in overall ezrin phosphorylation (Fig. 8 B) and a nearly complete elimination of microvilli (Fig. 8 C). In addition to accumulating at cell junctions and in the cytoplasm, expression of the LOK C-terminal domain caused and accumulated in long protrusive F-actin–containing structures devoid of ezrin mostly emanating from the basolateral membrane, suggesting the possibility that it imparts additional defects (Fig. 8 D). Expression of the equivalent region of SLK promoted a similar reduction in pERM as well as the loss of microvilli (Fig. S3, C and E, bottom). Surprisingly, expression of full-length kinase-dead LOK was much less efficient at reducing the number of cells with microvilli (Fig. 7 C), suggesting that the strong inhibitory effect of the C-terminal domain is partially masked in the context of the full-length protein.

At low levels of expression in the rare cells that have normal microvilli, the smaller fragment of the LOK C-terminal domain, LOK-586–968-GFP, localized preferentially to the distal ends of microvilli (Fig. 8 E). In individual microvilli, the intensities of ezrin and LOK-586–968-GFP display a partially mutually exclusive relationship along microvilli (Figs. 8, E and F; and S5 A). This phenomenon is not observed with full-length LOK (Fig. S5 B) and therefore appears to represent targeted inhibition of ezrin accumulation in discrete regions. Furthermore, because LOK-586–968-GFP is typically more concentrated on the tip than at the base of microvilli (Figs. 8, E and F; and S5 A), these results hint that endogenous kinase activity may be directed toward the growing distal tip of microvilli.

Discussion

Functional polarity requires the targeting of appropriate membrane proteins to specific domains but also defining the morphology of the domain by cytoplasmic factors, about which little is known. Here, we uncover how ezrin function is restricted to the apical membrane. We first demonstrate that phosphocycling on T567 is critical. Second, we identify the relevant kinases in epithelial cells as LOK and SLK. Third, we show that the kinases are enriched in microvilli through their C-terminal domain. Fourth, we show that the kinases are locally activated in microvilli.

Extensive characterization of the ERM phosphomimetic corresponding to ezrin T567D/E has shown that it reflects the activated form (Matsui et al., 1999; Polesello et al., 2002; Speck et al., 2003; Chambers and Bretscher, 2005; Charras et al., 2006; Carreno et al., 2008; Kunda et al., 2008). Earlier studies of epithelial cells suggested that overexpressing the ezrin phosphomimetic can provide more numerous microvilli, but these studies were performed in the presence of endogenous ezrin (Gautreau et al., 2000; Fievet et al., 2004). In contrast, we show that expression of the phosphomimetic in the absence of endogenous ezrin, unopposed phosphorylation of ezrin, or ezrin phosphorylated by a nonlocalized kinase all lead to its mislocalization to the basolateral membrane and the loss of its function. Our results are consistent with the finding in fly photoreceptor cells that reexpression of wild-type moesin restores apical microvilli after *moesin* gene disruption, whereas reexpression of phosphomimetic T559D moesin does not (Karagiosis and Ready, 2004).

We find that the normal ezrin phosphorylation cycle is ∼2 min, which is similar to the turnover rate as measured by

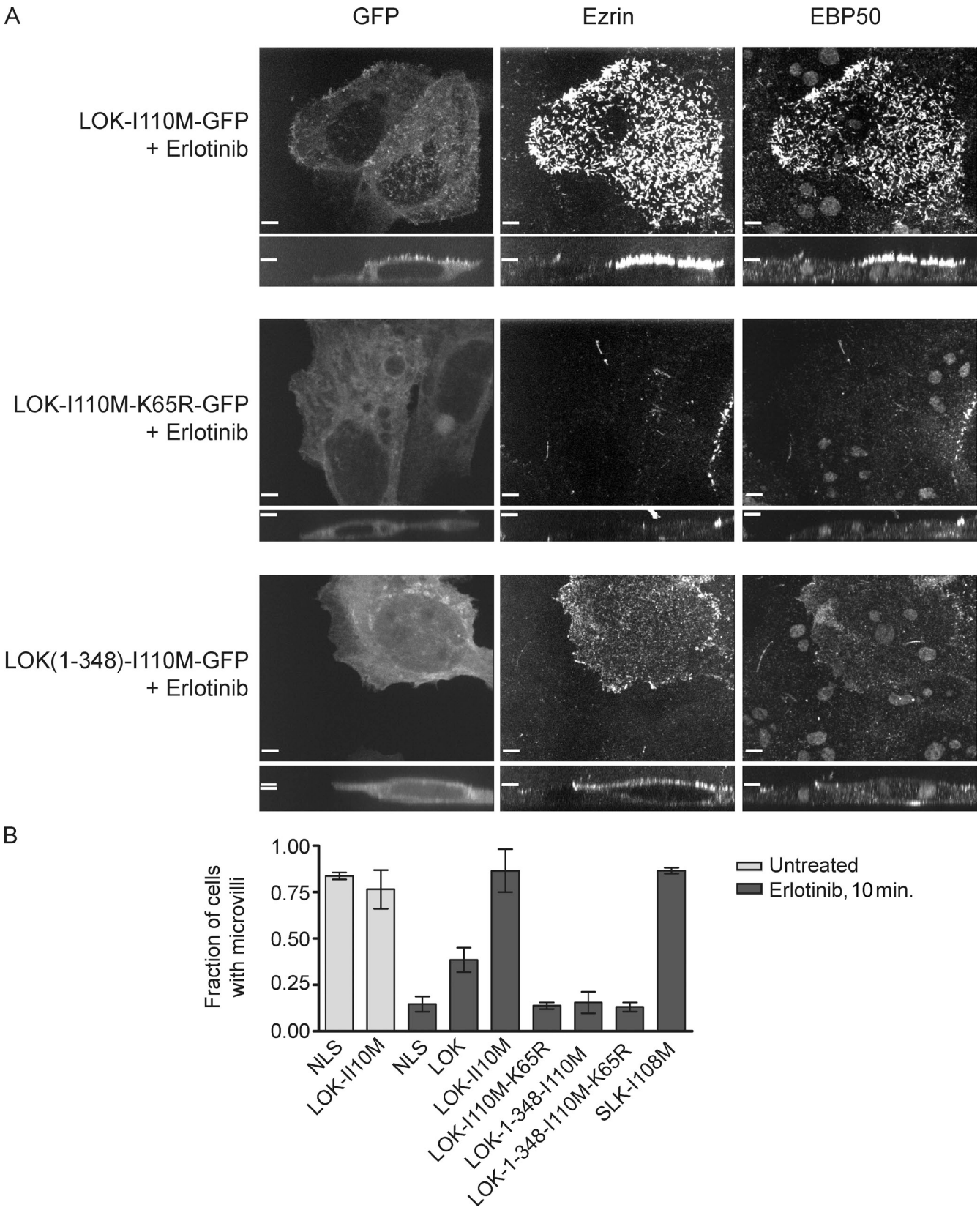

Figure 7. **Regulated LOK activity is necessary and sufficient for microvilli in the presence of erlotinib.** (A) Cells expressing erlotinib-resistant mutants of LOK as indicated were treated with 20 µM erlotinib for 10 min. LOK-I110M-GFP–transfected cells (or SLK-I108M-GFP–transfected cells; Fig. S4, B and C), but not neighboring untransfected cells, are protected from microvillus loss caused by erlotinib. Cells transfected with LOK-1–348-I110M-GFP have membrane-enriched depolarized ezrin but do not form microvilli. (B) Microvilli scoring of EBP50-stained Jeg-3 cells transfected with the indicated GFP-tagged protein or GFP-NLS as indicated and then treated with or without erlotinib. Data are means ± SD of three independent experiments. Bars, 10 µm.

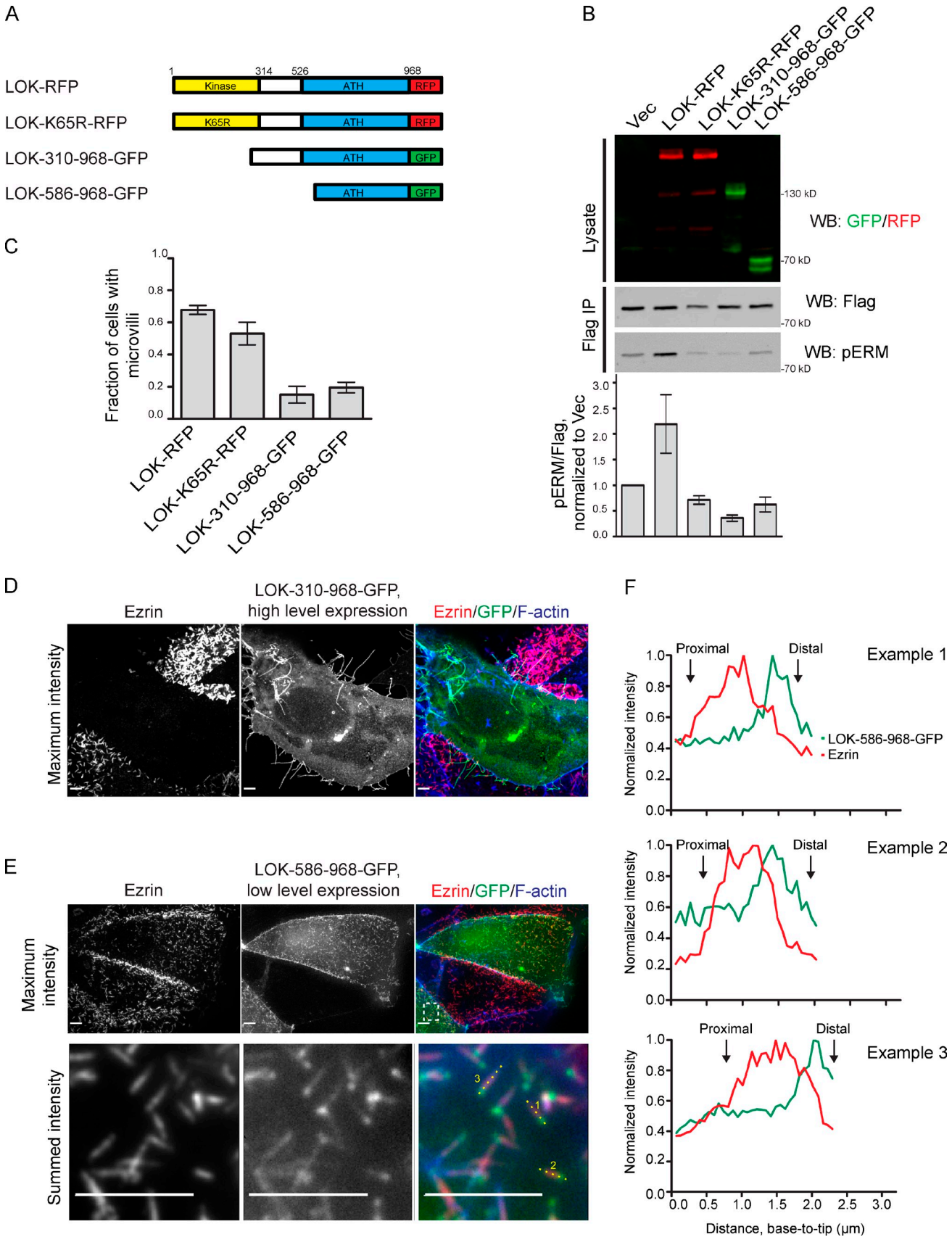

Figure 8. **Overexpression of the LOK C-terminal domain inhibits membrane association of ezrin, and this effect can be limited to extremely small regions within microvilli.** (A) Schematic of tagged truncation constructs used. ATH, AT1-46 homology. (B) Cells were cotransfected with empty vector (Vec) or GFP or RFP fusions of LOK along with ezrin-iFlag. The cells were lysed, ezrin-iFlag was immunoprecipitated with anti-iFlag (Flag IP), and phosphorylation

FRAP of ezrin-GFP in the same cells (Garbett and Bretscher, 2012). Thus, our data imply that the apical membrane is a dynamic system of local ezrin phosphorylation. Because microvilli have been shown to undergo constant remodeling (Gorelik et al., 2003; Garbett and Bretscher, 2012), phosphocycling ensures that activated ezrin can be recruited into growing microvilli as needed.

To identify the relevant kinases for ezrin T567 phosphorylation, we used an unbiased proteomic approach, leading us to LOK and SLK, two evolutionary homologues, which we found are necessary and sufficient for microvilli formation by localized ezrin. LOK has previously been shown to regulate moesin in lymphocytes. However, mice with the LOK gene knocked out have reduced ERM phosphorylation and alterations in chemokine-stimulated lymphocyte migration and polarization, but the mice are viable (Belkina et al., 2009). We suspect that in such knockout mice, SLK is providing a compensating function, and predict that a double LOK and SLK knockout mouse would be inviable. Because the ERM kinase in *Drosophila* is Slik, the homologue of LOK and SLK, this implies that regulation of ERM proteins by this family of kinases has an ancient evolutionary origin.

Earlier work has shown that in single epithelial Ls174T-W4 cells, a signal transduction pathway from LKB1/Strad results in the activation of the kinase MST4 to phosphorylate ezrin necessary for morphological assembly of the apical domain (ten Klooster et al., 2009; Gloerich et al., 2012). Moreover, these studies reported that phosphomimetic ezrin targets and restores microvilli in these MST4 knockdown cells, in apparent contradiction to our work. Although the expression level of phosphomimetic ezrin relative to endogenous ezrin was not reported, these results suggest that other mechanisms may exist under some circumstances to polarize ezrin apically. Furthermore, ten Klooster et al. (2009) also reported that knockdown of MST4 in Caco-2 cells induced defects in apical morphology (ten Klooster et al., 2009). In contrast, we have found that knockdown of LOK and SLK, but not MST4, in either Jeg-3 or Caco-2 results in reduced ezrin phosphorylation and loss of apical microvilli. We can offer no simple explanation for the difference in results between our and these studies.

Although both LOK in mammalian lymphocytes and *Drosophila* Slik have been implicated in ERM phosphorylation, it was not known how their function was restricted to a specific domain. We now show that the C-terminal region of both LOK and SLK target the kinase to apical microvilli and restrict their activity apically. Accordingly, overexpression of the LOK C-terminal domain uncoupled from the kinase domain acts as a dominant negative to inhibit ERM phosphorylation, leading to the destruction of microvilli. We find a similar effect in colon epithelial Caco-2 cells and kidney epithelial LLC-PK1.CL4 cells (unpublished data), suggesting that the mechanism by which LOK and SLK are regulated is general among epithelial cells.

We have previously shown that phosphoezrin and -radixin are enriched toward the tip of the microvillus and suggested that ezrin is phosphorylated at the microvillus tip and then moves down with treadmilling actin (Hanono et al., 2006). We now find a region within the LOK protein, which, when expressed at low levels, is often confined to the tip of microvilli, as would be expected if it is the relevant kinase. We therefore propose that some factor enriched at the microvillus tip recruits LOK and activates it there locally. Ezrin becomes phosphorylated, and as it moves down the microvillus, it begins to become dephosphorylated by a cytoplasmic phosphatase and ultimately releases from the membrane and F-actin at the base.

Interestingly, ERM anchorage has been invoked as a means for maintaining the protein composition of the apical domain in the absence of polarized membrane trafficking (Meder et al., 2005). The phosphocycling mechanism we describe, and thus polarized LOK/SLK, may therefore be a critical component of this "preapical" polarity pathway.

The work presented here has uncovered local regulation of ERM proteins by LOK and SLK through an unidentified microvillar component. So far, no interactors of LOK are known, but several binding partners of SLK have been reported, including microtubules (Wagner et al., 2002, 2008; Burakov et al., 2005), F-actin (Sabourin et al., 2000), PDZ domain–containing protein PDZK1 (Gisler et al., 2003), and the transcription factors Lbd1/2 (Storbeck et al., 2009). Our current efforts are aimed at determining whether these or other interactors are responsible for the polarized activity of LOK and SLK.

Materials and methods

Reagents, cDNAs, and siRNAs

Phos-tag reagent (Wako Chemicals USA) was added at 50 µM to standard Tris-glycine-SDS polyacrylamide gels according to the manufacturer's recommendations. Calyculin A and staurosporine were obtained from Enzo Life Sciences. Erlotinib was obtained from Cayman Chemical.

Ezrin antibodies were either a mouse antiezrin antibody (CPCT-ezrin-1 supernatant concentrate obtained from the Developmental Studies Hybridoma Bank developed under the auspices of the Eunice Kennedy Shriver National Institute of Child Health and Human Development and maintained by The University of Iowa Department of Biology) used at 1:5,000 (Western blot) or 1:100 (immunofluorescence) or a previously characterized rabbit polyclonal antibody raised against full-length human ezrin (Bretscher, 1989) and used at 1:5,000 (Western blot) or 1:300 (immunofluorescence). Rabbit antiradixin (raised against full-length, bacterially expressed radixin; Shcherbina et al., 1999) used at 1:50 (immunofluorescence) and rabbit anti-pERM (raised against recombinant phosphopeptide CRDKYK(pT)LRQIR; Matsui et al., 1998;

of ezrin-iFlag was detected by Western blotting and quantified. When the LOK C-terminal domain is overexpressed without an active kinase domain, ezrin-iFlag phosphorylation is inhibited. (C) Cells expressing the indicated LOK-GFP or -RFP fusions were stained for ezrin and F-actin and assessed for the presence of microvilli. LOK fusions that cause decreased pERM also cause microvillus loss. (D) Cells expressing high levels of the LOK C-terminal domain (LOK-310–968-GFP) were stained for ezrin and F-actin. The overexpression of the LOK C-terminal domain causes the loss of microvilli and formation of F-actin–positive protrusions lacking ezrin. (E) Cells expressing a low level of the shorter region of the LOK C-terminal domain (LOK-586–968-GFP) were stained for ezrin and F-actin. Bottom images show an enlargement of the region boxed in the top right image. (F) Fluorescence intensity along the lines indicated in E of three microvilli from their proximal to distal ends as marked. The minimal overexpression of the LOK C-terminal region often causes a loss of ezrin staining from the distal ends of microvilli. Data in B and C are means ± SD of three independent experiments. Data in F are representative of three replicates. WB, Western blot. Bars, 10 µm.

Hanono et al., 2006) used at 1:500 (Western blot) or 1:200 (immunofluorescence) have also been previously described. Rabbit anti-LOK used at 1:500 (Western blot) and rabbit anti-SLK used at 1:100 (Western blot) were purchased from Bethyl Laboratories, Inc. Mouse anti-Flag used at 1:5,000 (Western blot) or 1:100 (immunofluorescence) and mouse antitubulin used at 1:20,000 (Western blot) were obtained from Sigma-Aldrich. Mouse anti–E-cadherin used at 1:5,000 (Western blot) was obtained from BD. Rabbit anti-TagRFP used at 1:500 (Western blot) was purchased from Evrogen. Mouse anti-GFP used at 1:500 (Western blot) was obtained from Santa Cruz Biotechnology, Inc. Mouse anti-MST4 used at 1:5,000 (Western blot) was obtained from Epitomics.

To generate human ezrin cDNA resistant to siEzrin, four silent mutations (c612t, t615c, c618t, and g621a) were introduced into the ezrin ORF (Gary and Bretscher, 1995) by inverse tailored PCR. T567E mutant ezrin was a gift from J. Thoms (Cornell University, Ithaca, NY). For creation of stable cell lines, the pQCXIP vector (BD) was used. To generate pQCXIP/ezrin or pQCXIP/ezrin-iFlag and derivatives, ezrin cDNA was further mutated, and the eight-residue Flag tag (Fig. S1 C) was substituted by overlapping or inverse tailored PCR, respectively, and then subcloned into pQCXIP (BD). Ezrin-iFlag truncations were generated by PCR and subcloned into pQCXIP. For ezrin-GFP expression, ezrin cDNA was first cloned into pEGFP-N2, and then, the ezrin-GFP cassette was subcloned by tailored PCR into pQCXIP. The linking region between ezrin and GFP encoded the following peptide sequence: EFCSRRYRGPGIHRPVAT. LOK and truncations thereof were generated by tailored PCR using whole cDNA, which was made using mRNA isolated from Jeg-3 cells and the reverse transcriptase kit (SuperScript III; Invitrogen), a gift from J. Wayt (Cornell University, Ithaca, NY), and subcloned into pDONR221 by BP recombination (Invitrogen). They were then transferred into modified pcDNA-DEST vectors (Invitrogen) encoding C-terminal EGFP, C-terminal TagRFP-T, or C-terminal TagRFP-T-talin-1958–1241 by LR recombination (Invitrogen). The linking region between the ORF and the tags encoded the following peptide sequence: YPAFLYKVVRSR. Talin was cloned by PCR from Jeg-3 cDNA. The murine long isoform of SLK and truncations thereof were amplified by PCR from EST no. BC131675 purchased from Thermo Fisher Scientific and then cloned into pDONR223 by BP recombination. They were then transferred into the same set of modified pcDNA-DEST vectors by LR recombination, with one exception: SLK-310–1233 was transferred into pcDNA-DEST53 (Invitrogen), which adds an N-terminal (rather than C-terminal) GFP because this resulted in higher expression of this construct. Kinase-dead (K65R for LOK and K63R for SLK) mutations were generated using the mutagenesis kit (QuikChange; Agilent Technologies). For kinase assays, a C-terminal Flag tag was added to the 3′ end by tailored PCR of LOK-GFP or SLK-GFP and derivatives, and the products were cloned into pQCXIP. GST-ezrin-474–585 was previously described (Gary and Bretscher, 1995).

siRNAs were Validated Silencer Select from Ambion with the following sequences: 5′-GGAAUCAACUAUUUCGAGAdTdT-3′ (ezrin), 5′-GAAGAGCAUCGGAACCAGAdTdT-3′ (LOK, sequence 1), 5′-GGACUACACCAGGUUCCAAdTdT-3′ (LOK, sequence 2), 5′-GAUCGAUAUCUUUACAAGAdTdT-3′ (SLK, sequence 1), 5′-GCAGAAACAGACUAUCGAAdTdT-3′ (SLK, sequence 2), 5′-GCUUUACCACCGUACGAAAdTdT-3′ (MST4), and 5′-GAAUCCCGCUGACAAACCAdTdT-3′ (MINK1). siGL2, targeting GL2 luciferase (5′-CGUACGCGGAAUACUUCGAdTdT-3′), was previously described (Hanono et al., 2006).

Cell culture and cDNA/siRNA transfections

Jeg-3 cells (American Type Culture Collection) were maintained in a 5% CO_2 humidified atmosphere at 37°C in MEM (Invitrogen) with 10% FBS (Invitrogen). Caco-2 cells were maintained in MEM with 20% FBS. All transient plasmid DNA transfections used polyethylenimine reagent (PolyPlus) by forming complexes of DNA–polyethylenimine at a ratio of 2.5:1 and then adding 0.3 µg DNA to each centimeter squared of 30–50% confluent Jeg-3 cells (Hanono et al., 2006). Phoenix-Ampho retrovirus producer cells (American Type Culture Collection) were cultured in DMEM (Invitrogen) with 10% FBS. Retroviruses were prepared by transfecting the Phoenix-Ampho cell lined with pQCXIP and derivatives using Lipofectamine 2000 (Invitrogen) according to the manufacturer's protocol. The recombinant retroviruses were used to transduce Jeg-3 cells, which were then selected with 2.0 µg/ml puromycin (Sigma-Aldrich). For stable isotope labeling of amino acids in cell culture, cells expressing ezrin-iFlag or empty vector were grown for ≥2 wk in MEM (Thermo Fisher Scientific) containing dialyzed FBS (Invitrogen) and either C-13 arginine and lysine or C-12 arginine and lysine (Sigma-Aldrich), respectively.

All siRNAs were transfected at 30 nM into ∼25% confluent cultures of Jeg-3 cells or Caco-2 cells using Lipofectamine RNAiMAX (Invitrogen) using the manufacturer's protocol. In Fig. 5 B (fourth lane), cells were transfected with a mixture of 15 nM LOK and 15 nM SLK siRNAs. In all but one case, cells were processed for immunofluorescence or lysis 3 d after transfection. In Fig. 4 C, cells were treated with the indicated first siRNA for 2 d, reseeded, and then, on the third day, transfected with the indicated second siRNA for an additional 3 d and processed on the sixth day.

Immunoprecipitations and mass spectrometry

LOK and SLK interaction was determined by cross-linking immunoprecipitation. In brief, before lysis, cells were treated with warm PBS containing 1.25 mM dithiobis(succinimidylpropionate) (Thermo Fisher Scientific), a cell-permeable, thiol-reversible cross-linking agent, for 2 min at 37°C. Excess cross-linker was quenched by extensive washing in TBS for 15 min at room temperature. Cells were then solubilized in cold immunoprecipitation buffer (25 mM Tris, pH 7.4, 5% glycerol, 150 mM NaCl, 50 mM NaF, 0.1 mM Na_3VO_4, 10 mM β-glycerol phosphate, 8.7 mg/ml paranitrophenylphosphate, 0.5% Triton X-100, 0.1 µM calyculin A, and protease inhibitor tablet [Roche]) and immunoprecipitated for 2 h using Flag M2 affinity gel (Sigma-Aldrich). For Western blots, immunoprecipitates were extensively washed in immunoprecipitation wash buffer (25 mM Tris, pH 7.4, 5% glycerol, 150 mM NaCl, 50 mM NaF, and 0.2% Triton X-100) and then eluted in 200 µg/ml 3×Flag peptide, denatured in Laemmli buffer, resolved by SDS-PAGE, transferred to polyvinylidene difluoride, and then interrogated with specific antibodies.

For mass spectrometry, we followed a protocol adapted from Smolka et al. (2007) and Albuquerque et al. (2008). In brief, immunoprecipitates were eluted in 50 mM Tris, pH 8.0, and 1% SDS and then precipitated with 49.9% acetone, 50% ethanol, and 0.1% acetic acid. Proteins were digested with trypsin (Promega) and desalted in a C18 column (Waters). After drying the peptides in a speed vac, the sample was dissolved in 80% acetonitrile and 1% formic acid and fractionated by hydrophilic interaction chromatography. Resulting fractions were dried, dissolved in 0.1% trifluoroacetic acid, and injected into a mass spectrometer (Orbitrap XL; Thermo Fisher Scientific). The data were analyzed using a Sorcerer system (Sage-N) running Sequest for protein identification and Xpress for peptide quantitation. Interacting proteins were limited to serine/threonine kinases for which at least three peptides were identified with a peptide probability score >0.9 and a heavy versus light enrichment >2.0.

For analysis of tagged ezrin phosphorylation, cells transfected with ezrin-iFlag plasmid plus LOK or SLK expression vector were rapidly boiled in 50 mM Tris, pH 8.0, containing 1% SDS. Lysates were then diluted 10-fold with immunoprecipitation buffer and clarified, and the protein abundance was quantified and adjusted using the 660-nm Protein Assay (Thermo Fisher Scientific), and immunoprecipitated as described in the previous paragraph.

Western blotting and densitometry

Western blots were performed as previously described (Hanono et al., 2006). For all densitometry, Western blotting was performed with a mixture of mouse CPCT-ezrin-1 or mouse Flag and rabbit pERM antibodies, detected with infrared fluorescent secondary antibodies (Invitrogen or LI-COR Biosciences). Membranes were imaged using a scanner (Odyssey; LI-COR Biosciences). On every membrane in this study, dilutions of lysate were run alongside the samples so that standard curves for both total ezrin and pERM could be generated in the Odyssey software. These were then used to determine the relative intensity of in-range pERM and ezrin or Flag signals from experimental lanes. These data were exported to Prism software (GraphPad Software) in which all further quantitative and statistical analyses were performed.

Immunofluorescence and image analysis

Cells grown on glass coverslips were fixed in 3.7% formalin/PBS for 15 min at room temperature for all experiments except in Figs. S3 B and S4 C, in which cells were fixed in cold 10% trichloroacetic acid for 15 min as previously described (Hayashi et al., 1999). Cells were then washed with PBS and blocked with immunofluorescence buffer (PBS + 0.5% BSA + 0.5% goat serum + 0.1% Triton X-100) for 10 min. Primary and secondary antibodies were then applied in immunofluorescence buffer containing 1% FBS. Alexa Fluor–conjugated phalloidin (Invitrogen), to stain F-actin, was added to the secondary as required. The cells were mounted in Vectashield reagent (Vector Laboratories), imaged using a spinning-disk microscope (CSU-X; Intelligent Imaging Innovations) with spherical aberration correction device, 63×, 1.4 NA objective on a microscope (DMI6000 B; Leica), acquired with either an electron-multiplying charge-coupled device camera (QuantEM; Photometrics) or a charge-coupled device camera (HQ2; Photometrics) using SlideBook software (Intelligent Imaging Innovations).

Maximum or summed intensity projections were assembled in SlideBook and exported to Illustrator software (Adobe). For clarity, side projections were vertically expanded fivefold using Illustrator.

The presence or absence of microvilli was scored as described previously (Hanono et al., 2006; Garbett et al., 2010; LaLonde et al., 2010). More than 200 cells per replicate were stained using the indicated antibody or phalloidin and binned into three categories: microvilli, no microvilli, or abnormal. As mentioned in the text, microvilli above cell–cell junctions were ignored in the scoring. Abnormal cells represented <10% of cells scored and did not change as a result of the experimental treatments in this study.

For scoring of ezrin localization to the basolateral domain induced by delocalized LOK expression, the cell middle or cell base was identified by confocal microscopy using F-actin staining for 50 transfected cells per sample per trial, and the presence or absence of ezrin stain in transfected cells relative to surrounding nontransfected cells was reported. For line intensity analysis, a line was drawn along a single microvillus from base to tip (the orientation was verified by scanning through multiple z sections), and the intensities of ezrin immunofluorescent staining, GFP, and F-actin were each calculated in SlideBook and exported into Excel software (Microsoft). Ezrin and GFP were each divided by F-actin to minimize aberrations in microvilli geometry, and the resulting data were plotted in Prism.

Kinase assays

Kinase assays were essentially as previously described (Jackson and Dickson, 1999). GST-ezrin-474–585 was purified from Rosetta2(DE3)pLysS bacteria (EMD Millipore) onto glutathione agarose (Sigma-Aldrich) and then washed extensively in TBS. pQCXIP plasmids encoding kinase constructs were transiently transfected into Phoenix-Ampho cells for ∼18 h, cells were Flag immunoprecipitated in immunoprecipitation buffer for 2 h, and the resin was extensively washed in TBS. Immunoprecipitates were eluted in TBS containing 200 µg/ml 3×Flag peptide and quickly resolved by SDS-PAGE to verify purity and determine concentration. Approximately 0.2 µM GST-ezrin-474–585 beads were added to ∼0.2 µM soluble kinase in kinase assay buffer (150 mM NaCl, 20 mM Tris, pH 7.4, 50 mM $MnCl_2$, 100 mM $MgCl_2$, 0.1 µM Na_3VO_4, 0.1 µM calyculin A, and 20 µM ATP), and the reactions were incubated at 30°C for 1 h with agitation and then terminated by boiling in Laemmli buffer.

Online supplemental material

Fig. S1 further validates the specificity of ezrin T567 phosphorylation and the use of tagged ezrin. Fig. S2 shows that in Jeg-3 cells, endogenous LOK can be coimmunoprecipitated with ezrin-iFlag and confirms that RNAi of LOK causes a reduction in ezrin phosphorylation with a second siRNA sequence, whereas RNAi of MINK1 or MST4 has no effect. Fig. S3 examines phosphoezrin/radixin distribution in cells transfected with the LOK N-terminal kinase domain and also shows that identical effects to those shown in Figs. 6 and 8 with LOK truncations result from overexpression of SLK truncations. Fig. S4 illustrates our rational design of erlotinib-resistant LOK and that resistant SLK protects cells from erlotinib-induced microvillus collapse and examines pERM distribution in such cells. Fig. S5 examines additional microvilli from cells transfected with LOK-586–968-GFP as well as microvilli from cells expressing full-length LOK-GFP. Online supplemental material is available at http://www.jcb.org/cgi/content/full/jcb.201207047/DC1.

We are grateful to Dr. Abraham Hanono for the ezrin cross-linking immunoprecipitation protocol, Dr. Julie Thoms for construction of ezrin phosphomutants, Jessica Wayt for Jeg-3 cDNA, and Dr. Volker Vogt for advice regarding stable cell line creation. We also thank members of the Bretscher laboratory for critically reading this manuscript and Dr. Yuxin Mao for help with structural analysis.

This work was supported by National Institutes of Health grant GM-036652 to A. Bretscher. R. Viswanatha and P.Y. Ohouo were partially supported by National Institutes of Health Training grant 5T32GM007273.

Submitted: 6 July 2012
Accepted: 6 November 2012

References

Albuquerque, C.P., M.B. Smolka, S.H. Payne, V. Bafna, J. Eng, and H. Zhou. 2008. A multidimensional chromatography technology for in-depth phosphoproteome analysis. *Mol. Cell. Proteomics*. 7:1389–1396. http://dx.doi.org/10.1074/mcp.M700468-MCP200

Belkina, N.V., Y. Liu, J.J. Hao, H. Karasuyama, and S. Shaw. 2009. LOK is a major ERM kinase in resting lymphocytes and regulates cytoskeletal rearrangement through ERM phosphorylation. *Proc. Natl. Acad. Sci. USA*. 106:4707–4712. http://dx.doi.org/10.1073/pnas.0805963106

Bonilha, V.L., S.C. Finnemann, and E. Rodriguez-Boulan. 1999. Ezrin promotes morphogenesis of apical microvilli and basal infoldings in retinal pigment epithelium. *J. Cell Biol.* 147:1533–1548. http://dx.doi.org/10.1083/jcb.147.7.1533

Bonilha, V.L., M.E. Rayborn, I. Saotome, A.I. McClatchey, and J.G. Hollyfield. 2006. Microvilli defects in retinas of ezrin knockout mice. *Exp. Eye Res.* 82:720–729. http://dx.doi.org/10.1016/j.exer.2005.09.013

Bretscher, A. 1989. Rapid phosphorylation and reorganization of ezrin and spectrin accompany morphological changes induced in A-431 cells by epidermal growth factor. *J. Cell Biol.* 108:921–930. http://dx.doi.org/10.1083/jcb.108.3.921

Burakov, A.V., O.V. Kovalenko, E.S. Potekhina, E.S. Nadezhdina, and L.A. Zinovkina. 2005. LOSK (SLK) protein kinase activity is necessary for microtubule organization in the interphase cell centrosome. *Dokl. Biol. Sci.* 403:317–319. http://dx.doi.org/10.1007/s10630-005-0123-9

Carreno, S., I. Kouranti, E.S. Glusman, M.T. Fuller, A. Echard, and F. Payre. 2008. Moesin and its activating kinase Slik are required for cortical stability and microtubule organization in mitotic cells. *J. Cell Biol.* 180:739–746. http://dx.doi.org/10.1083/jcb.200709161

Chambers, D.N., and A. Bretscher. 2005. Ezrin mutants affecting dimerization and activation. *Biochemistry*. 44:3926–3932. http://dx.doi.org/10.1021/bi0480382

Charras, G.T., C.K. Hu, M. Coughlin, and T.J. Mitchison. 2006. Reassembly of contractile actin cortex in cell blebs. *J. Cell Biol.* 175:477–490. http://dx.doi.org/10.1083/jcb.200602085

Chen, J., J.A. Cohn, and L.J. Mandel. 1995. Dephosphorylation of ezrin as an early event in renal microvillar breakdown and anoxic injury. *Proc. Natl. Acad. Sci. USA*. 92:7495–7499. http://dx.doi.org/10.1073/pnas.92.16.7495

Crepaldi, T., A. Gautreau, P.M. Comoglio, D. Louvard, and M. Arpin. 1997. Ezrin is an effector of hepatocyte growth factor–mediated migration and morphogenesis in epithelial cells. *J. Cell Biol.* 138:423–434. http://dx.doi.org/10.1083/jcb.138.2.423

Coscoy, S., F. Waharte, A. Gautreau, M. Martin, D. Louvard, P. Mangeat, M. Arpin, and F. Amblard. 2002. Molecular analysis of microscopic ezrin dynamics by two-photon FRAP. *Proc. Natl. Acad. Sci. USA*. 99:12813–12818. http://dx.doi.org/10.1073/pnas.192084599

Dard, N., S. Louvet, A. Santa-Maria, J. Aghion, M. Martin, P. Mangeat, and B. Maro. 2001. In vivo functional analysis of ezrin during mouse blastocyst formation. *Dev. Biol.* 233:161–173. http://dx.doi.org/10.1006/dbio.2001.0192

Delpire, E. 2009. The mammalian family of sterile 20p-like protein kinases. *Pflugers Arch.* 458:953–967. http://dx.doi.org/10.1007/s00424-009-0674-y

Fehon, R.G., A.I. McClatchey, and A. Bretscher. 2010. Organizing the cell cortex: the role of ERM proteins. *Nat. Rev. Mol. Cell Biol.* 11:276–287. http://dx.doi.org/10.1038/nrm2866

Fidalgo, M., A. Guerrero, M. Fraile, C. Iglesias, C.M. Pombo, and J. Zalvide. 2012. Adaptor protein cerebral cavernous malformation 3 (CCM3) mediates phosphorylation of the cytoskeletal proteins ezrin/radixin/moesin by mammalian Ste20-4 to protect cells from oxidative stress. *J. Biol. Chem.* 287:11556–11565. http://dx.doi.org/10.1074/jbc.M111.320259

Fievet, B.T., A. Gautreau, C. Roy, L. Del Maestro, P. Mangeat, D. Louvard, and M. Arpin. 2004. Phosphoinositide binding and phosphorylation act sequentially in the activation mechanism of ezrin. *J. Cell Biol.* 164:653–659. http://dx.doi.org/10.1083/jcb.200307032

Finnerty, C.M., D. Chambers, J. Ingraffea, H.R. Faber, P.A. Karplus, and A. Bretscher. 2004. The EBP50-moesin interaction involves a binding site regulated by direct masking on the FERM domain. *J. Cell Sci.* 117:1547–1552. http://dx.doi.org/10.1242/jcs.01038

Garbett, D., and A. Bretscher. 2012. PDZ interactions regulate rapid turnover of the scaffolding protein EBP50 in microvilli. *J. Cell Biol.* 198:195–203. http://dx.doi.org/10.1083/jcb.201204008

Garbett, D., D.P. LaLonde, and A. Bretscher. 2010. The scaffolding protein EBP50 regulates microvillar assembly in a phosphorylation-dependent manner. *J. Cell Biol.* 191:397–413. http://dx.doi.org/10.1083/jcb.201004115

Gary, R., and A. Bretscher. 1995. Ezrin self-association involves binding of an N-terminal domain to a normally masked C-terminal domain that includes the F-actin binding site. *Mol. Biol. Cell*. 6:1061–1075.

Gautreau, A., D. Louvard, and M. Arpin. 2000. Morphogenic effects of ezrin require a phosphorylation-induced transition from oligomers to monomers at the plasma membrane. *J. Cell Biol.* 150:193–203. http://dx.doi.org/10.1083/jcb.150.1.193

Gisler, S.M., S. Pribanic, D. Bacic, P. Forrer, A. Gantenbein, L.A. Sabourin, A. Tsuji, Z.S. Zhao, E. Manser, J. Biber, and H. Murer. 2003. PDZK1: I. a

major scaffolder in brush borders of proximal tubular cells. *Kidney Int.* 64:1733–1745. http://dx.doi.org/10.1046/j.1523-1755.2003.00266.x

Gloerich, M., J.P. ten Klooster, M.J. Vliem, T. Koorman, F.J. Zwartkruis, H. Clevers, and J.L. Bos. 2012. Rap2A links intestinal cell polarity to brush border formation. *Nat. Cell Biol.* 14:793–801. http://dx.doi.org/10.1038/ncb2537

Gorelik, J., A.I. Shevchuk, G.I. Frolenkov, I.A. Diakonov, M.J. Lab, C.J. Kros, G.P. Richardson, I. Vodyanoy, C.R. Edwards, D. Klenerman, and Y.E. Korchev. 2003. Dynamic assembly of surface structures in living cells. *Proc. Natl. Acad. Sci. USA*. 100:5819–5822. http://dx.doi.org/10.1073/pnas.1030502100

Hanono, A., D. Garbett, D. Reczek, D.N. Chambers, and A. Bretscher. 2006. EPI64 regulates microvillar subdomains and structure. *J. Cell Biol.* 175:803–813. http://dx.doi.org/10.1083/jcb.200604046

Hayashi, K., S. Yonemura, T. Matsui, and S. Tsukita. 1999. Immunofluorescence detection of ezrin/radixin/moesin (ERM) proteins with their carboxyl-terminal threonine phosphorylated in cultured cells and tissues. *J. Cell Sci.* 112:1149–1158.

Hipfner, D.R., N. Keller, and S.M. Cohen. 2004. Slik Sterile-20 kinase regulates Moesin activity to promote epithelial integrity during tissue growth. *Genes Dev.* 18:2243–2248. http://dx.doi.org/10.1101/gad.303304

Hirao, M., N. Sato, T. Kondo, S. Yonemura, M. Monden, T. Sasaki, Y. Takai, S. Tsukita, and S. Tsukita. 1996. Regulation mechanism of ERM (ezrin/radixin/moesin) protein/plasma membrane association: possible involvement of phosphatidylinositol turnover and Rho-dependent signaling pathway. *J. Cell Biol.* 135:37–51. http://dx.doi.org/10.1083/jcb.135.1.37

Hughes, S.C., and R.G. Fehon. 2006. Phosphorylation and activity of the tumor suppressor Merlin and the ERM protein Moesin are coordinately regulated by the Slik kinase. *J. Cell Biol.* 175:305–313. http://dx.doi.org/10.1083/jcb.200608009

Jackson, D.I., and C. Dickson. 1999. Protein techniques. Immunoprecipitation, in vitro kinase assays, and western blotting. *Methods Mol. Biol.* 97: 699–708.

Karagiosis, S.A., and D.F. Ready. 2004. Moesin contributes an essential structural role in *Drosophila* photoreceptor morphogenesis. *Development*. 131:725–732. http://dx.doi.org/10.1242/dev.00976

Kinoshita, E., E. Kinoshita-Kikuta, K. Takiyama, and T. Koike. 2006. Phosphate-binding tag, a new tool to visualize phosphorylated proteins. *Mol. Cell. Proteomics*. 5:749–757.

Kunda, P., A.E. Pelling, T. Liu, and B. Baum. 2008. Moesin controls cortical rigidity, cell rounding, and spindle morphogenesis during mitosis. *Curr. Biol.* 18:91–101. http://dx.doi.org/10.1016/j.cub.2007.12.051

LaLonde, D.P., D. Garbett, and A. Bretscher. 2010. A regulated complex of the scaffolding proteins PDZK1 and EBP50 with ezrin contribute to microvillar organization. *Mol. Biol. Cell*. 21:1519–1529. http://dx.doi.org/10.1091/mbc.E10-01-0008

Li, Q., M.R. Nance, R. Kulikauskas, K. Nyberg, R. Fehon, P.A. Karplus, A. Bretscher, and J.J. Tesmer. 2007. Self-masking in an intact ERM-merlin protein: an active role for the central alpha-helical domain. *J. Mol. Biol.* 365:1446–1459. http://dx.doi.org/10.1016/j.jmb.2006.10.075

Matsui, T., M. Maeda, Y. Doi, S. Yonemura, M. Amano, K. Kaibuchi, S. Tsukita, and S. Tsukita. 1998. Rho-kinase phosphorylates COOH-terminal threonines of ezrin/radixin/moesin (ERM) proteins and regulates their head-to-tail association. *J. Cell Biol.* 140:647–657. http://dx.doi.org/10.1083/jcb.140.3.647

Matsui, T., S. Yonemura, S. Tsukita, and S. Tsukita. 1999. Activation of ERM proteins in vivo by Rho involves phosphatidyl-inositol 4-phosphate 5-kinase and not ROCK kinases. *Curr. Biol.* 9:1259–1262. http://dx.doi.org/10.1016/S0960-9822(99)80508-9

Meder, D., A. Shevchenko, K. Simons, and J. Füllekrug. 2005. Gp135/podocalyxin and NHERF-2 participate in the formation of a preapical domain during polarization of MDCK cells. *J. Cell Biol.* 168:303–313. http://dx.doi.org/10.1083/jcb.200407072

Nakamura, F., M.R. Amieva, C. Hirota, Y. Mizuno, and H. Furthmayr. 1996. Phosphorylation of 558T of moesin detected by site-specific antibodies in RAW264.7 macrophages. *Biochem. Biophys. Res. Commun.* 226:650–656. http://dx.doi.org/10.1006/bbrc.1996.1410

Nakamura, N., N. Oshiro, Y. Fukata, M. Amano, M. Fukata, S. Kuroda, Y. Matsuura, T. Leung, L. Lim, and K. Kaibuchi. 2000. Phosphorylation of ERM proteins at filopodia induced by Cdc42. *Genes Cells*. 5:571–581. http://dx.doi.org/10.1046/j.1365-2443.2000.00348.x

Ng, T., M. Parsons, W.E. Hughes, J. Monypenny, D. Zicha, A. Gautreau, M. Arpin, S. Gschmeissner, P.J. Verveer, P.I. Bastiaens, and P.J. Parker. 2001. Ezrin is a downstream effector of trafficking PKC-integrin complexes involved in the control of cell motility. *EMBO J.* 20:2723–2741. http://dx.doi.org/10.1093/emboj/20.11.2723

Ong, S.E., B. Blagoev, I. Kratchmarova, D.B. Kristensen, H. Steen, A. Pandey, and M. Mann. 2002. Stable isotope labeling by amino acids in cell culture, SILAC, as a simple and accurate approach to expression proteomics. *Mol. Cell. Proteomics*. 1:376–386. http://dx.doi.org/10.1074/mcp.M200025-MCP200

Pao, W., and J. Chmielecki. 2010. Rational, biologically based treatment of EGFR-mutant non-small-cell lung cancer. *Nat. Rev. Cancer*. 10:760–774. http://dx.doi.org/10.1038/nrc2947

Pao, W., V.A. Miller, K.A. Politi, G.J. Riely, R. Somwar, M.F. Zakowski, M.G. Kris, and H. Varmus. 2005. Acquired resistance of lung adenocarcinomas to gefitinib or erlotinib is associated with a second mutation in the EGFR kinase domain. *PLoS Med.* 2:e73. http://dx.doi.org/10.1371/journal.pmed.0020073

Pearson, M.A., D. Reczek, A. Bretscher, and P.A. Karplus. 2000. Structure of the ERM protein moesin reveals the FERM domain fold masked by an extended actin binding tail domain. *Cell*. 101:259–270. http://dx.doi.org/10.1016/S0092-8674(00)80836-3

Pietromonaco, S.F., P.C. Simons, A. Altman, and L. Elias. 1998. Protein kinase C-theta phosphorylation of moesin in the actin-binding sequence. *J. Biol. Chem.* 273:7594–7603. http://dx.doi.org/10.1074/jbc.273.13.7594

Polesello, C., I. Delon, P. Valenti, P. Ferrer, and F. Payre. 2002. Dmoesin controls actin-based cell shape and polarity during *Drosophila melanogaster* oogenesis. *Nat. Cell Biol.* 4:782–789. http://dx.doi.org/10.1038/ncb856

Sabourin, L.A., K. Tamai, P. Seale, J. Wagner, and M.A. Rudnicki. 2000. Caspase 3 cleavage of the Ste20-related kinase SLK releases and activates an apoptosis-inducing kinase domain and an actin-disassembling region. *Mol. Cell. Biol.* 20:684–696. http://dx.doi.org/10.1128/MCB.20.2.684-696.2000

Shcherbina, A., A. Bretscher, D.M. Kenney, and E. Remold-O'Donnell. 1999. Moesin, the major ERM protein of lymphocytes and platelets, differs from ezrin in its insensitivity to calpain. *FEBS Lett.* 443:31–36. http://dx.doi.org/10.1016/S0014-5793(98)01674-3

Simons, P.C., S.F. Pietromonaco, D. Reczek, A. Bretscher, and L. Elias. 1998. C-terminal threonine phosphorylation activates ERM proteins to link the cell's cortical lipid bilayer to the cytoskeleton. *Biochem. Biophys. Res. Commun.* 253:561–565. http://dx.doi.org/10.1006/bbrc.1998.9823

Smolka, M.B., C.P. Albuquerque, S.H. Chen, and H. Zhou. 2007. Proteome-wide identification of in vivo targets of DNA damage checkpoint kinases. *Proc. Natl. Acad. Sci. USA*. 104:10364–10369. http://dx.doi.org/10.1073/pnas.0701622104

Speck, O., S.C. Hughes, N.K. Noren, R.M. Kulikauskas, and R.G. Fehon. 2003. Moesin functions antagonistically to the Rho pathway to maintain epithelial integrity. *Nature*. 421:83–87. http://dx.doi.org/10.1038/nature01295

Storbeck, C.J., S. Wagner, P. O'Reilly, M. McKay, R.J. Parks, H. Westphal, and L.A. Sabourin. 2009. The Ldb1 and Ldb2 transcriptional cofactors interact with the Ste20-like kinase SLK and regulate cell migration. *Mol. Biol. Cell*. 20:4174–4182. http://dx.doi.org/10.1091/mbc.E08-07-0707

Takeuchi, K., N. Sato, H. Kasahara, N. Funayama, A. Nagafuchi, S. Yonemura, S. Tsukita, and S. Tsukita. 1994. Perturbation of cell adhesion and microvilli formation by antisense oligonucleotides to ERM family members. *J. Cell Biol.* 125:1371–1384. http://dx.doi.org/10.1083/jcb.125.6.1371

ten Klooster, J.P., M. Jansen, J. Yuan, V. Oorschot, H. Begthel, V. Di Giacomo, F. Colland, J. de Koning, M.M. Maurice, P. Hornbeck, and H. Clevers. 2009. Mst4 and Ezrin induce brush borders downstream of the Lkb1/Strad/Mo25 polarization complex. *Dev. Cell*. 16:551–562. http://dx.doi.org/10.1016/j.devcel.2009.01.016

Wagner, S., T.A. Flood, P. O'Reilly, K. Hume, and L.A. Sabourin. 2002. Association of the Ste20-like kinase (SLK) with the microtubule. Role in Rac1-mediated regulation of actin dynamics during cell adhesion and spreading. *J. Biol. Chem.* 277:37685–37692. http://dx.doi.org/10.1074/jbc.M205899200

Wagner, S., C.J. Storbeck, K. Roovers, Z.Y. Chaar, P. Kolodziej, M. McKay, and L.A. Sabourin. 2008. FAK/src-family dependent activation of the Ste20-like kinase SLK is required for microtubule-dependent focal adhesion turnover and cell migration. *PLoS ONE*. 3:e1868. http://dx.doi.org/10.1371/journal.pone.0001868

Xing, B., A. Jedsadayanmata, and S.C. Lam. 2001. Localization of an integrin binding site to the C terminus of talin. *J. Biol. Chem.* 276:44373–44378. http://dx.doi.org/10.1074/jbc.M108587200

Yamamoto, N., M. Honma, and H. Suzuki. 2011. Off-target serine/threonine kinase 10 inhibition by erlotinib enhances lymphocytic activity leading to severe skin disorders. *Mol. Pharmacol.* 80:466–475. http://dx.doi.org/10.1124/mol.110.070862

Yonemura, S., S. Tsukita, and S. Tsukita. 1999. Direct involvement of ezrin/radixin/moesin (ERM)-binding membrane proteins in the organization of microvilli in collaboration with activated ERM proteins. *J. Cell Biol.* 145:1497–1509. http://dx.doi.org/10.1083/jcb.145.7.1497